

# Comparative study of empirical force-field and DFT models of amorphous $\text{TiO}_2$ nanoparticles

Nicolas Gastellu<sup>1</sup> and Rustam Z. Khaliullin<sup>1,\*</sup>

<sup>1</sup>*Department of Chemistry, McGill University, 801 Sherbrooke St. West, Montreal, QC H3A 0B8, Canada*

(Dated: September 3, 2018)

We calculate the energy of the conformations of amorphous titania nanoparticles obtained in classical MD simulations at  $T = 300$  K using the classical two-body Matsui-Akaogi (MA) potential and Kohn-Sham density functional theory (DFT) in the Perdew-Burke-Ernzerhof approximation. Comparative analysis of the energies shows the values obtained using the MAP formalism are only weakly correlated with those calculated with DFT. Remarkably we also found that a simple rutile nanocrystal (RZK: is this a nanocrystal? it is supposed to be perfect periodic lattice), for which the MA potential is expected to be well-parameterized, exhibited almost no correlation between the two sets of calculated energies. We discuss possible reasons for this discrepancy and examine implications of our results, chief among them is the suitability of the classical MA potential for amorphous titania nanoparticles.

## INTRODUCTION

Titania ( $\text{TiO}_2$ ) has long been the subject of notable research interest due to its high chemical stability and interesting optical, dielectric, mechanical, and photocatalytic properties<sup>1–4</sup>. While most works focus on  $\text{TiO}_2$  in its most stable and common forms, which are all crystalline, a number of technological uses of this material rely on processing into film or powder form which both tend to be amorphous; further modification of the material is then needed to restore it to a certain level of crystalline order<sup>5,6</sup>. Dependence on this last step makes titania significantly more difficult and expensive to use in industrial-scale applications, which has motivated researchers to study amorphous  $\text{TiO}_2$  ( $a - \text{TiO}_2$ ) in hope of being able to use in it cheaper, less processed forms<sup>7–9</sup>.

One of the defining traits of amorphous materials is their lack of long-range order, which makes their microstructure hard to study experimentally. In spite of this, recent experimental studies have been successful in describing the local atomic structure of  $a - \text{TiO}_2$  under different environments<sup>10–12</sup> by measuring structural properties such as the coordination number of bulk and surface Ti atoms and average bond lengths, using various types of X-ray absorption structure spectroscopy. However, the most detailed investigations of amorphous titania's structure have been those combining experimental methods (e.g. X-ray absorption spectroscopy) with the computation modeling (notably reverse Monte-Carlo simulations)<sup>13–15</sup>. Our reliance on simulations to properly understand this material is a major research incentive for theoretical chemists to devise the adequate computational tools.

While computational chemistry software employs a miscellany of procedures to generate results, one can distinguish two main approaches to running such calculations:

- the classical approach, which uses a predetermined potential  $V(\mathbf{r}_1, \dots, \mathbf{r}_N)$  and Newton's equations of motion to calculate the trajectories and energies of

all atoms in the simulation,

- the *ab-initio* approach, which relies on a quantum mechanical description (usually density functional theory, or DFT) of the system to determine its electronic density from which all other physical quantities are then derived.

DFT is generally considered more accurate than empirical force-field calculations, due to its more faithful description of interactions between each atoms in the system being studied. Unfortunately, DFT calculations on large systems ( $\sim 1000$  atoms) are much more difficult to implement due to the prohibitive amounts of memory needed and long computation times. Researchers have therefore put considerable effort into developing classical potentials that faithfully reproduce experimental measurements which could allow accurate simulations of  $\text{TiO}_2$  (notably) without resorting to computationally expensive calculations<sup>16–18</sup>. The potential devised by Matsui and Akaogi in 1991<sup>17</sup> has had notable success in describing the structural and mechanical properties of titania's different polytypes<sup>19,20</sup> and is thus the most widely used potential when simulating  $\text{TiO}_2$  using classical MD. In this work, we focus our attention on nanoparticulate  $a - \text{TiO}_2$  (such as can be found in unprocessed powder form) and on whether this classical potential can accurately predict their structure-energy relationship, or potential energy surface (PES)  $V(\mathbf{r}_1, \dots, \mathbf{r}_N)$ . We compare the energies yielded by the classical and quantum descriptions of the system to see how well correlated they are. In this report, we describe our different calculation methods, then we present and discuss our results, before introducing potential directions for future research.

## I. COMPUTATIONAL METHODS

The open-source atomistic simulations package CP2K<sup>21</sup> was used to run all calculations and simulations presented in this work.

### A. Obtaining nanoparticle structures

We generated the atomic structures of  $a$ -TiO<sub>2</sub> nanoparticles using a series of classical MD simulations. All classical MD simulations discussed below were ran in the  $NpT$  ensemble, using the Matsui-Akaogi (MA) two-body potential (see next section) to model the interactions between pairs of atoms. The atomic structures of the various  $a$ -TiO<sub>2</sub> nanoparticles described in this work were obtained in multiple steps, using the melt-quenching method employed by a number of computational studies of amorphous materials<sup>6,22</sup>. We started by melting rutile ( $r$ -TiO<sub>2</sub>) nanocrystals of 198, 390, and 768 atoms respectively whose structures were previously optimized *via* DFT at the BLYP/DZVP level of theory (with a plane-wave energy cutoff of 2100 Ry) using classical MD in the  $NpT$  ensemble with  $T = 2000$  K and  $p_{\text{ext},0} = 0.0$  Pa. We ran this first round of simulations for 40000 timesteps of  $\Delta t = 0.5$  fs. The resulting melt was then cooled in three steps; classical MD simulations using the same potentials, ensemble, and number of steps were ran using  $T = 1500$  K, 750 K, and 300 K successively, all with  $\Delta t = 2.0$  fs. This process simulated the annealing of the melted nanocrystals into a glass. Having obtained equilibrated atomic structures for nanoparticles of different sizes, we sampled 101 conformations from the last 40 ps of the last cooling run, at which point all four nanoparticles were in equilibrium with the  $T = 300$  K thermal bath.

Seeing as the MA potential was originally elaborated to describe the structural and elastic properties of bulk  $r$ -TiO<sub>2</sub>, we also generated a set of conformations of a rutile lattice comprised of 72 atoms in the  $NpT$  ensemble at  $T = 300$  K, using periodic boundary conditions to avoid surface effects. Doing so provided us with energy values which we expect to be well correlated with the ones we obtain with DFT methods, thus giving us a reference data set to which we could compare the rest of our results.

### B. Empirical potential

The MA potential was originally developed for classical MD simulations of the four main polytypes of crystalline TiO<sub>2</sub><sup>17</sup> to accurately simulate the structural properties of titania's four main polytypes and the elastic constants of rutile ( $r$ -TiO<sub>2</sub>). It is the most widely used potential when classically simulating bulk TiO<sub>2</sub> and has been shown by previous studies<sup>19,20,23</sup> to be the most adequate force field for predicting the structure and properties of its liquid and amorphous phases. The MA potential describes the short-range interaction between atoms with a Buckingham potential and their long-range elec-

TABLE I. Parameters used for evaluating the MA potentials.

Element	$Z$ ( $ e $ )	$A$ (Å)	$B$ (Å)	$C$ (Å <sup>3</sup> kJ <sup>1/2</sup> mol <sup>-1/2</sup> )
Ti	+2.196	1.1823	0.077	22.5
O	-1.098	1.6339	0.117	54.0

trostatic interaction using the traditional Coulomb term:

$$V_{ij}(r) = f_0 \cdot (B_i + B_j) \cdot \exp\left(\frac{A_i + A_j - r}{B_i + B_j}\right) - \frac{C_i C_j}{r^6} + \frac{e Z_i Z_j}{4\pi\epsilon_0 r}, \quad (1)$$

where  $r$  denotes the distance between the two interacting ions  $i$  and  $j$ ,  $e$  is the elementary charge,  $Z_i$  is the dimensionless ionic charge of ion  $i$ ,  $f_0$  is a standard force of 4.184 kJ·mol<sup>-1</sup>Å<sup>-1</sup>, and  $A_i$ ,  $B_i$ , and  $C_i$  are parameters corresponding to species  $i$ . The charges  $Z_{\text{Ti}}$  and  $Z_{\text{O}}$  were obtained from Traylor *et al.*<sup>24</sup>, who derived them from phonon dispersion curves observed in rutile ( $r$ -TiO<sub>2</sub>). The numerical values of the other constants listed above were determined by Matsui and Akaogi by adjusting them adjusting them to reproduce the observed elastic constants of rutile and fitting them to reproduce the structures of rutile, brookite, and anatase (the three polytypes of crystalline titania for which precise experimental measurements of lattice parameters were available at the time of their paper). These values are given in table I. The total potential energy of the system is then given by the sum of all pairwise interactions between all of its  $N$  atoms:

$$V(\mathbf{r}_1, \dots, \mathbf{r}_N) = \sum_{i < j}^N V_{ij}(|\mathbf{r}_i - \mathbf{r}_j|). \quad (2)$$

### C. DFT calculations

We ran a single-point energy calculation on each conformation using traditional Kohn-Sham (KS) DFT in the generalised gradient approximation (GGA), with the fully non-empirical functional developed by Perdew, Burke, and Ernzerhof<sup>25</sup> (i.e. the PBE functional). We employed a double-zeta valence polarised (DZVP) basis set, with a plane-wave cutoff of 2000 Ry. This was all implemented using CP2K's Quickstep module for DFT calculations<sup>26</sup>. We also ran similar DFT calculations on the different configurations of the reference rutile lattice which we also sampled from the last 40 ps of the MD simulation we mentioned in the last paragraph of the last section.

Seeing as core electrons have been shown to have a negligible impact on the interatomic interactions in TiO<sub>2</sub><sup>15,27</sup> (especially at  $p = 0$  Pa), we used norm-conserving pseudopotentials developed by Goedecker, Teter, and Hutter<sup>28</sup> to avoid having to explicitly account for them in our electronic density optimisation routine, thereby making our *ab-initio* calculations significantly

computationally cheaper. The GTH pseudopotentials used in this study treated oxygen's  $1s$  orbitals as part of its core and included all but titanium's  $3p$ ,  $3d$ , and  $4s$  electrons into titanium's core.

## II. RESULTS AND DISCUSSION

### A. Accuracy of KS DFT results

Before discussing the accuracy of our classically obtained energy values, we must first establish the accuracy of our DFT energy values for each system, since these values will serve as references to which we will compare the energies returned by the classical MD simulation. One of the main reasons why we expect our DFT results to be more realistic than the ones yielded by the classical MD simulations is that DFT's quantum formalism is better suited to describe systems at an atomic scale than the classical picture. Indeed, while classical mechanics remain a valid description of macroscopic systems (containing  $\sim 10^{24}$  atoms), they do not apply to the behaviour of individual atoms, which are quantum objects (i.e. do not evolve deterministically and thus have to be described using time-evolving probability distributions). Seeing as both methods implemented in this work describe the forces in amorphous  $\text{TiO}_2$  nanoparticles atom by atom, it is safe to assume that the procedure rooted in the most accurate theoretical substrate for describing microscopic systems yields better results. Furthermore, classical MD simulation rely on a fixed expression for the system's PES, whose parameters are empirically determined and thus subject to experimental error. Another problem with the potential we used for our classical MD runs is the fact that its parameters been tailored to reproduce the structures and properties of crystalline titania whereas we are trying to verify its accuracy for  $a - \text{TiO}_2$ .

Going beyond merely conceptual arguments for assuming that our DFT results are more accurate than those we obtained using classical MD, we note that KS DFT has been extensively used to study amorphous and crystalline titania in various forms and environments with good success<sup>6,27,29,30</sup>. DFT methods thus have a proven track record of correctly reproducing experimentally observed properties, which further comforts our assumption that the energy values we calculating using DFT are a good reference to which we can compare our classical results.

### B. Comparing classical MD with KS DFT

For each nanoparticle, we compare the classically evaluated energy of every configuration with the energy obtained through a DFT calculation for that some configuration. We plot our results in figures 2-6; a  $y = x$  line was added to every plot to give a better appreciation of the level of correlation between classical and DFT data

sets. This allows us to gauge the accuracy of MA force-field; if the classical and quantum mechanical results are well correlated, then the purely classical representation of the forces in the nanoparticles is sufficiently accurate to discriminate between slight variations in a given system's configuration in a meaningful way and can therefore be used to simulate this system nanoparticles instead of DFT, which is much more computationally expensive.

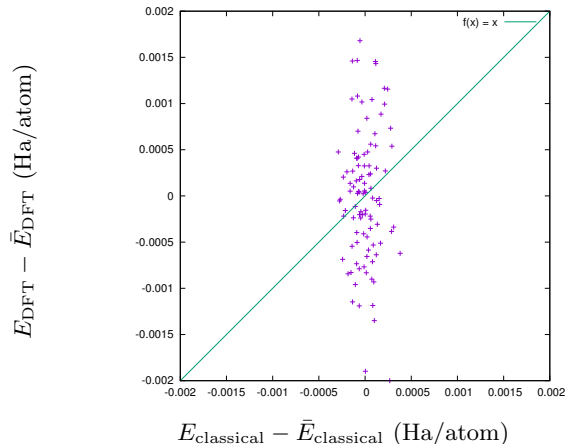


FIG. 1. DFT energy vs. classical energy (both shifted down by their average value) for 101 conformations of an  $r - \text{TiO}_2$  lattice with 72 atoms.

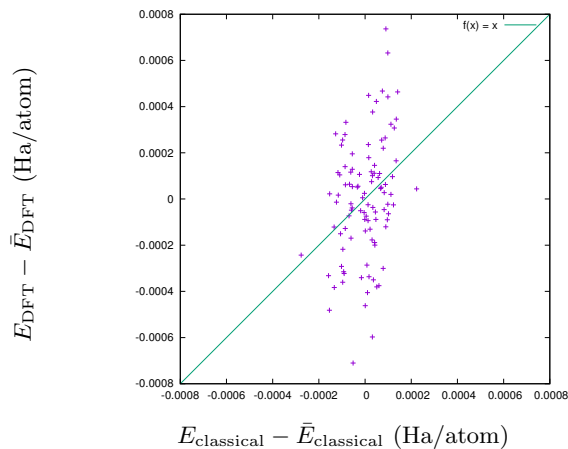


FIG. 2. DFT energy vs. classical energy (both shifted down by their average value) for 101 conformations of an  $a - \text{TiO}_2$  nanoparticle with 198 atoms.

Comparing the energies obtained using classical MD and those calculated using DFT reveals that a description of the forces inside an  $a - \text{TiO}_2$  nanoparticle using only the two-body MA potential is not precise enough to yield an accurate representation of its PES. Indeed, plotting the energies yielded by both calculation methods reveals that DFT calculation methods are much more sensitive to a change in a given nanoparticle's

atomic configuration than classical methods.

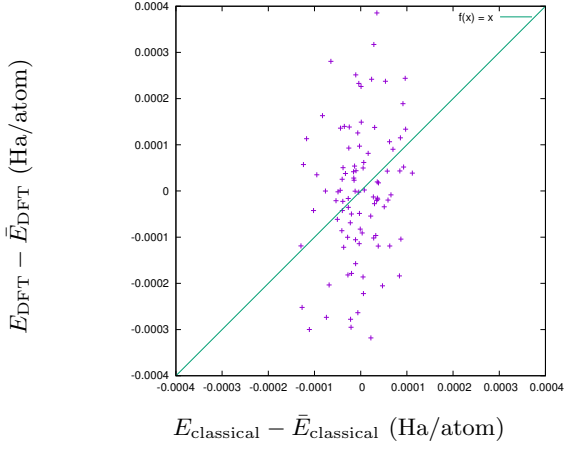


FIG. 3. DFT energy vs. classical energy (both shifted down by their average value) for 101 conformations of an  $a$ -TiO<sub>2</sub> nanoparticle with 390 atoms.

The system for which this is the most obvious is the 768 atom nanoparticle, for which all classically evaluated energies lie within  $\sim 10^{-4}$  Ha of each other, while the energies obtained using quantum mechanical methods vary by  $\sim 10^{-1}$  Ha. One can get a sense of how dramatic this disparity between the ranges of both data sets by examining figure 4: when plotting the DFT and classical data on the same scale, the classical energy values almost all lie on the same vertical line and thus appear to all be identical. While this effect is most dramatic for the 768 atom system, every other nanoparticle on which we ran similar calculations exhibit significant clustering of the energies obtained using the MA potential about their mean value, while their DFT energies spread out over a much larger interval.

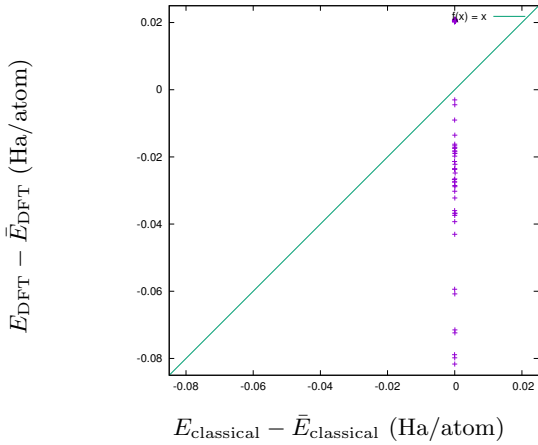


FIG. 4. DFT energy vs. classical energy (both shifted down by their average value) for 101 conformations of an  $a$ -TiO<sub>2</sub> nanoparticle with 768 atoms.

All four systems we ran these calculations on exhibit weak correlation between the DFT-calculated energy values and the energies obtained using the MA potential. Even more surprisingly, we find that the two sets of energy values of the different conformations of the rutile lattice were even less correlated than the ones obtained from the amorphous nanoparticles. As can be seen in table II B, our simulated rutile lattice yielded the lowest value of  $\rho$  of all the systems we studied.

In light of this extremely low correlation, we cannot consider our simulated  $r$ -TiO<sub>2</sub> lattice a reference system. This unexpectedly poor correlation between these two sets of energy values also questions the accuracy of our DFT results, which have been our accuracy benchmark throughout this paper.

Assuming that our DFT calculations are indeed accurate, this lack of correlation between the energies obtained from  $r$ -TiO<sub>2</sub> is not overly problematic; it could simply suggest that a purely classical two-body description of atomic interactions in TiO<sub>2</sub> in the amorphous or rutile phase is not sufficiently accurate to keep track of small changes in the system's configuration. Moreover the small RMSE values we get for all systems (except the 768-atom nanoparticle) and the fact that all classically obtained energies for a given system are very close to each other suggest that they are still physically sound at a less precise level of analysis. If both sets of energy values for each system varied over intervals of similar sizes and yet remained as uncorrelated as we have observed them to be, then the validity of trying to describe TiO<sub>2</sub> using only the MA potential would be seriously questioned. However this is not the case; for every system all energies computed classically differ very little. This is consistent with the fact that the atomic configurations from which such energies are computed were obtained from segments of our MD simulations where the system was already at equilibrium with its environment (i.e. the thermal bath) and thus did not vary greatly either. It is therefore reassuring to see that, within our classical MD simulation, snapshots which have similar structures are also found to have close energy values. The contrast between the highly clustered classical values and the much more spread out quantum values could therefore suggest that the quantum description of TiO<sub>2</sub> is much more sensitive to the system's conformational changes while using the MA potential cannot meaningfully register such changes yet still provides an internally consistent and physically viable picture of the system. This is further suggested by other works which only used the MA potential to model TiO<sub>2</sub> (in both amorphous and crystalline states) and have successfully reproduced a number of experimental findings on the local atomic structure of the systems being considered<sup>20,23,31</sup>. Interpreting our findings in this light would lead us to the conclusion that while the MA picture is sufficient to meaningfully describe some of titania's structural properties, one would still need DFT to properly describe its electronic structure and its related characteristics (e.g. magnetic behaviour, dielectric

constant, etc.).

As we have seen, there is a serious discrepancy between the PES predicted by the MA force-field and that predicted by DFT. While this is hardly surprising, the difference between both models' respective PESs raises some interesting problems when trying to directly compare the energy of a particular arrangement of atoms given by both methods. We obtained our structures from MD simulations that used the MA potential and allowed the atomic configurations of our different systems to equilibrate with the thermal bath of each run. We are therefore running all of our energy calculations on conformations sampled from the region surrounding a local minimum of the MA PES of our different systems, which implies that these conformations' MA energies will all be very close to one another ( $|\nabla^N V_{\text{classical}}| \sim 0$  near a minimum of the classical PES). This will not be the case for the energies we obtain using DFT because MA-obtained atomic configurations do not lie near a local minimum of the PES predicted by DFT. We can therefore expect  $|\nabla^N V_{\text{DFT}}|$  to be non-negligible for those conformations, thus leading to large differences in DFT-computed energies from one configuration to the next. This is exactly what we observe for both crystalline and amorphous titania. Figure 5 shows a schematic explanation of how this disagreement between the two PESs yields the clustered values we observe in our MA energy sets and the disperse values characteristic of our DFT energy sets. For simplicity, both the  $3N$ -dimensional PESs obtained are represented as unidimensional and are assumed to be harmonic with local minima located near one another (i.e. functions of the form of  $V(x) = k \cdot (x - x_0)^2$ ). As the figure clearly shows, two qualitatively similar PESs with slightly different topologies can yield energy values that are poorly correlated uncorrelated.

Our method of directly comparing the energies of individual conformations is therefore overly naive. A better way to compare the accuracy of DFT with the MA force-field would be to generate structures using both methods instead of comparing the energies of structures obtained solely using classical MD using the MA potential. One could then compare the structural properties (e.g. density, average bond lengths, etc.) of both sets of configurations to their experimentally observed values and determine which method yields the most precise predictions. A sketch-map<sup>32</sup> algorithm could also be used to judge the similarity between DFT-obtained structures and those generated by the MA potential. The proportion of conformations obtained through both methods that are alike would give us another indicator of the level of agreement between both models.

Surface effects could also be an important factor responsible for the uncorrelatedness of our  $a - \text{TiO}_2$  energy values. As previously stated, the MA potential was developed to reproduce the bulk structures of  $\text{TiO}_2$  in its various crystalline forms; the potential was developed by simulating nanocrystals ranging from 384 atoms to 576 atoms in size and the bulk properties of the dif-

ferent crystalline polytypes of titania were used to fix its energy parameters<sup>17</sup>. Knowing that the surface sites of a  $\text{TiO}_2$  nanoparticle (crystalline or amorphous) have significantly different atomic and electronic structures as bulk sites<sup>20,29,31</sup>, it is easy to see how a model built to simulate systems containing mainly bulk sites can reach erroneous results when trying reproduce a nanoparticle with a significant portion of its atoms on the surface. It is probable that conducting a similar study on set of larger  $a - \text{TiO}_2$  nanoparticles would yield better correlated classical and DFT energy values. Unfortunately, running DFT single-point energy calculations on larger nanoparticles might prove to be prohibitively computationally expensive without optimising the DFT calculation scheme to handle systems with many atoms ( $> 1000$  atoms).

Computational expense being one of DFT's main drawbacks, a number of optimisation schemes have been proposed over the years to reduce both the amount of memory and the time necessary to run calculations on large systems ( $\sim 1000$  atoms). Among them, the absolutely localised molecular orbitals<sup>33</sup> (ALMO) method partitions the simulated system into small fragments (usually the individual atoms or molecules that compose it) and runs traditional DFT on each fragment in parallel. This has the advantage of having a runtime that scales linearly with the number of fragments for large systems, while traditional DFT calculation runtimes scale cubically with the number of atoms being simulated. Seeing as ALMO DFT makes a number of large DFT calculations much more feasible, it would allow us to conduct a similar study on larger nanoparticles (with more bulk sites) which could potentially yield better correlated classical and DFT values. This could furthermore enable us to run simulations of nanoparticles with sizes closer to those of  $a - \text{TiO}_2$  nanoparticles used in most practical applications ( $\sim 4 \text{ nm}$ <sup>29</sup>) and therefore give us a better appreciation of how the MA potential performs on systems it is better adapted to model.

Another way to run similar calculations on larger  $\text{TiO}_2$  nanoparticles would be use smaller basis sets. While the basis set we used to describe oxygen's electronic distribution (DZVP) cannot be further reduced without removing a polarisation function (which is crucial to adequately describe chemical bonding), the basis set we used for Ti explicitly describes the electrons in its three highest occupied subshells ( $3p$ ,  $3d$ , and  $4s$ ). Knowing that we can safely assume that titanium's six  $3p$  electrons have negligible impact on bonding in  $\text{TiO}_2$ <sup>27</sup>, we can use a basis set and pseudopotential which treat them as core electrons. This would significantly reduce the memory cost and computation time of a DFT simulation of any system containing numerous Ti atoms, thus making DFT calculations on large  $\text{TiO}_2$  nanoparticles more easily implementable.

Regardless of how well the MA potential describes  $r - \text{TiO}_2$ , the data we obtained from modeling amorphous systems unequivocally indicates that the pic-

System	$a - \text{TiO}_2$ (198 atoms)	$a - \text{TiO}_2$ (390 atoms)	$a - \text{TiO}_2$ (768 atoms)	$r - \text{TiO}_2$ (72 atoms)
$\rho$	0.3066474	0.3497706	-0.0496755	0.0141203
RMSE	0.0486056	0.0628487	22.21090	0.0518275

TABLE II. Pearson correlation coefficient  $\rho$  and RMSE between the energy values obtained through DFT and those obtained using the two-body MA potential on various configurations of different systems.

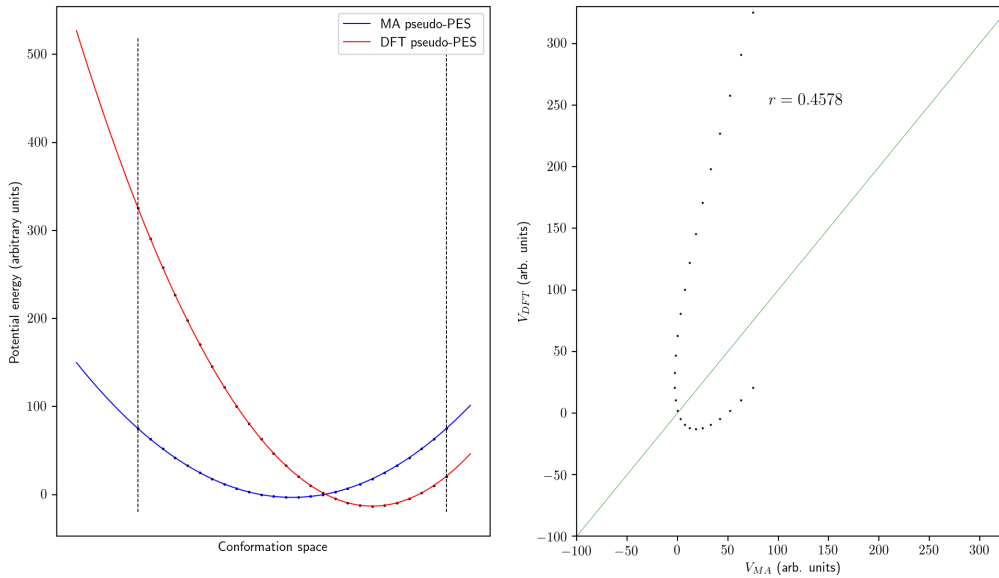


FIG. 5. Schematic representation of the problems arising from direct comparison of energy values yielded by differing PESs. In the left-hand plot both PESs are assumed to be 1-dimensional (instead of depending on the  $3N$  position variables of the system's  $N$  atoms). We can see how conformations (black dots) sampled near the minimum of the MA PES (blue curve) are much more spread out in energy when projected on the PES obtained using DFT (red curve), yielding a similar comparison to the one drawn by our data. The right-hand scatter plot presents the energies obtained from both PESs in the same way we plotted the actual energy values obtained from our calculations, and  $r$  denotes the Pearson correlation coefficient between both sets of sampled energies.

ture of  $\text{TiO}_2$  provided by the MA potential is not consistent with DFT's description of the material.

## CONCLUSION

Our comparison of the energy values we obtained through DFT and those calculated with the classical MA potential, on common sets of conformations of various  $\text{TiO}_2$  nanoparticles has consistently revealed that these two data sets are weakly correlated. These results imply that the PES of a small  $a - \text{TiO}_2$  predicted by the MA force-field is significantly different from the one produced by KS DFT. Having established our DFT results to be more accurate than the ones yielded by the MA potential, we can safely assume that the MA potential does not faithfully reproduce the PES of small titania nanoparticles. This holding true even for the set of energies obtained from a system which we believed to be well-described by both methods – a 72-atom ru-

tile lattice – raises some questions about the validity of our methods and calls for further research into this topic. The observed discrepancy between the PESs yielded by both models invalidates our approach of comparing the energies of different atomic configurations directly to one another; it fails to account for the change in topology between both energy surfaces thus making both methods appear more disparate than they might truly be.

Conducting classical and DFT simulations on larger nanoparticles could also provide further insight, since the structure and properties of large nanoparticles are less impacted by their surface sites than smaller nanoparticles<sup>29</sup>. This motivates the development of cheaper, more scalable DFT schemes. Being able to carry out such calculations on large systems could eventually allow for full MD simulations of nanoparticulate titania using DFT. This would give researchers the means to generate atomic structures of  $\text{TiO}_2$  nanoparticles from first principles only. Comparing these *ab-initio* structures' properties (e.g. density, bulk/surface coordination

number, average bond length) to those of structures obtained through experiment or using classical potentials might also offer insight on how well-suited both simulations methods are to describing such systems. Implementations of DFT that are optimised for large systems could also be used to study the size dependence of many of nanoparticulate titania's properties and to examine whether our current models can adequately account for them.

This work therefore raises more questions than it answers. Fortunately, the problems posed by our results leave us with a clear sense of what needs to be done to further elucidate the level of accuracy of classical MD simulations of amorphous titania. The main axes of future research we propose is the modelisation of larger, more practically relevant nanoparticles and the use of linear scaling DFT routines to simulate such nanoparticles from first principles.

- 
- \* rustam.khaliullin@mcgill.ca
- <sup>1</sup> P. A. Christensen, A. Dilks, T. A. Egerton, and J. Temperley, "Infrared spectroscopic evaluation of the photodegradation of paint part ii: The effect of uv intensity & wavelength on the degradation of acrylic films pigmented with titanium dioxide," *Journal of Materials Science* **35**, 5353–5358 (2000).
  - <sup>2</sup> K.A. Vorotilov, E.V. Orlova, and V.I. Petrovsky, "Sol-gel tio2 films on silicon substrates," *Thin Solid Films* **207**, 180 – 184 (1992).
  - <sup>3</sup> AJ Perry and HK Pulker, "Hardness, adhesion and abrasion resistance of tio2 films on glass," *Thin Solid Films* **124**, 323–333 (1985).
  - <sup>4</sup> Yi Ma, Xiuli Wang, Yushuai Jia, Xiaobo Chen, Hongxian Han, and Can Li, "Titanium dioxide-based nanomaterials for photocatalytic fuel generations," *Chemical reviews* **114**, 9987–10043 (2014).
  - <sup>5</sup> Hengbo Yin, Yuji Wada, Takayuki Kitamura, Shingo Kambe, Sadao Murasawa, Hirotaro Mori, Takao Sakata, and Shozo Yanagida, "Hydrothermal synthesis of nano-sized anatase and rutile tio2 using amorphous phase tio2," *Journal of Materials Chemistry* **11**, 1694–1703 (2001).
  - <sup>6</sup> Binay Prasai, Bin Cai, M. Kylee Underwood, James P. Lewis, and D. A. Drabold, "Properties of amorphous and crystalline titanium dioxide from first principles," *Journal of Materials Science* **47**, 7515–7521 (2012).
  - <sup>7</sup> Jian Zou, Jiacheng Gao, and Fengyu Xie, "An amorphous tio2 sol sensitized with h2o2 with the enhancement of photocatalytic activity," *Journal of Alloys and Compounds* **497**, 420–427 (2010).
  - <sup>8</sup> Miki Kanna, Sumpun Wongnawa, Supat Buddee, Ketsarin Dilokkhunakul, and Peerathat Pinpithak, "Amorphous titanium dioxide: a recyclable dye remover for water treatment," *Journal of sol-gel science and technology* **53**, 162–170 (2010).
  - <sup>9</sup> Hu Young Jeong, Jeong Yong Lee, and Sung-Yool Choi, "Interface-engineered amorphous tio2-based resistive memory devices," *Advanced Functional Materials* **20**, 3912–3917 (2010).
  - <sup>10</sup> Vittorio Luca, Samitha Djajanti, and Russell F Howe, "Structural and electronic properties of sol-gel titanium oxides studied by x-ray absorption spectroscopy," *The Journal of Physical Chemistry B* **102**, 10650–10657 (1998).
  - <sup>11</sup> Hideaki Yoshitake, Tae Sugihara, and Takashi Tatsumi, "Xafs study on the local structure of ti in amorphous mesoporous titania," *Physical Chemistry Chemical Physics* **5**, 767–772 (2003).
  - <sup>12</sup> Marcos Fernández-García, Carolina Belver, Jonathan C Hanson, Xianqin Wang, and José A Rodriguez, "Anatase-tio2 nanomaterials: Analysis of key parameters controlling crystallization," *Journal of the American Chemical Society* **129**, 13604–13612 (2007).
  - <sup>13</sup> V Petkov, G Holzhüter, U Tröge, Th Gerber, and B Himmel, "Atomic-scale structure of amorphous tio2 by electron, x-ray diffraction and reverse monte carlo simulations," *Journal of non-crystalline solids* **231**, 17–30 (1998).
  - <sup>14</sup> Hengzhong Zhang, Bin Chen, Jillian F Banfield, and Glenn A Waychunas, "Atomic structure of nanometer-sized amorphous tio 2," *Physical Review B* **78**, 214106 (2008).
  - <sup>15</sup> C. A. Triana, C. Moyses Araujo, R. Ahuja, G. A. Niklasson, and T. Edvinsson, "Electronic transitions induced by short-range structural order in amorphous tio2," *Phys. Rev. B* **94**, 165129 (2016).
  - <sup>16</sup> Dae-Weon Kim, Naoya Enomoto, Zenbe-e Nakagawa, and Katsuyuki Kawamura, "Molecular dynamic simulation in titanium dioxide polymorphs: Rutile, brookite, and anatase," *Journal of the American Ceramic Society* **79**, 1095–1099 (1996).
  - <sup>17</sup> Masanori Matsui and Masaki Akaogi, "Molecular dynamics simulation of the structural and physical properties of the four polymorphs of tio2," *Molecular Simulation* **6**, 239–244 (1991).
  - <sup>18</sup> Erik G Brandt and Alexander P Lyubartsev, "Systematic optimization of a force field for classical simulations of tio2–water interfaces," *The Journal of Physical Chemistry C* **119**, 18110–18125 (2015).
  - <sup>19</sup> DR Collins and W Smith, *Daresbury Research Report DL-TR-96-001: Evaluation of TiO2 forcefields.*, Tech. Rep. (Council for the Central Laboratory of Research Councils, 1996).
  - <sup>20</sup> Vo Van Hoang, "Structural properties of simulated liquid and amorphous tio2," *physica status solidi (b)* **244**, 1280–1287 (2007).
  - <sup>21</sup> CP2K Developers Group, "2K open source molecular dynamics: www.cp2k.org," (—2018—).
  - <sup>22</sup> DA Drabold, "Topics in the theory of amorphous materials," *The European Physical Journal B* **68**, 1–21 (2009).
  - <sup>23</sup> Mozghan Alimohammadi and Kristen A Fichthorn, "Molecular dynamics simulation of the aggregation of titanium dioxide nanocrystals: preferential alignment," *Nano letters* **9**, 4198–4203 (2009).
  - <sup>24</sup> Joseph Gibson Traylor, HG Smith, RM Nicklow, and MK Wilkinson, "Lattice dynamics of rutile," *Physical Review B* **3**, 3457 (1971).
  - <sup>25</sup> J. P. Perdew, K. Burke, and M. Ernzerhof, "Generalized gradient approximation made simple," *Phys. Rev. Lett.* **77**, 3865 (1996).
  - <sup>26</sup> J. Vandevondele, M. Krack, F. Mohamed, M. Parrinello, T. Chassaing, and J. Hutter, "Quickstep: Fast and accu-

- rate density functional calculations using a mixed gaussian and plane waves approach,” *Comput. Phys. Commun.* **167**, 103 (2005).
- <sup>27</sup> M Landmann, E Rauls, and WG Schmidt, “The electronic structure and optical response of rutile, anatase and brookite tio<sub>2</sub>,” *Journal of physics: condensed matter* **24**, 195503 (2012).
- <sup>28</sup> S Goedecker, M Teter, and Jürg Hutter, “Separable dual-space gaussian pseudopotentials,” *Physical Review B* **54**, 1703 (1996).
- <sup>29</sup> Daniele Selli, Gianluca Fazio, and Cristiana Di Valentin, “Using density functional theory to model realistic tio<sub>2</sub> nanoparticles, their photoactivation and interaction with water,” *Catalysts* **7**, 357 (2017).
- <sup>30</sup> E Shojaei and MR Mohammadizadeh, “First-principles elastic and thermal properties of tio<sub>2</sub>: a phonon approach,” *Journal of Physics: Condensed Matter* **22**, 015401 (2009).
- <sup>31</sup> VV Hoang, Hoang Zung, and Ngo Huynh Buu Trong, “Structural properties of amorphous tio<sub>2</sub> nanoparticles,” *The European Physical Journal D* **44**, 515–524 (2007).
- <sup>32</sup> Michele Ceriotti, Gareth A Tribello, and Michele Parrinello, “Simplifying the representation of complex free-energy landscapes using sketch-map,” *Proceedings of the National Academy of Sciences* **108**, 13023–13028 (2011).
- <sup>33</sup> Rustam Z Khaliullin, Joost VandeVondele, and Jurg Hutter, “Efficient linear-scaling density functional theory for molecular systems,” *Journal of chemical theory and computation* **9**, 4421–4427 (2013).